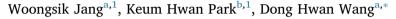
Contents lists available at ScienceDirect

Organic Electronics

journal homepage: www.elsevier.com/locate/orgel

Increased omnidirectional light absorbance by using hollow silica nanoparticles in an anti-reflective pattern for efficient organic photovoltaic devices



^a School of Integrative Engineering, Chung-Ang University, 84 Heukseok-Ro, Dongjak-gu, Seoul, 06974, Republic of Korea ^b Display Components & Materials Research Center, Korea Electronics Technology Institute, Saenari-ro, Bundang-gu, Seongnam-si, Gyeonggi-do, 13509, Republic of Korea

ARTICLE INFO

Keywords: Anti-reflection coating Hollow silica nanoparticles Low refractive index Organic solar cells Angle-of-incidence

ABSTRACT

We investigated a single-layer low refractive index anti-reflection (AR) coating on an organic photovoltaic device, using hollow silica nanoparticles, as shown in a cross-sectional TEM image. The PCE (6.53%) of the device with the AR pattern layer was improved, which contributed to the increased light absorption in the broadband range and charge generation at normal incidence observed by optical and electrical analysis, respectively. Comparing the photovoltaic performance of the devices without and with the AR pattern layer by hollow silica nanoparticles, the AR pattern achieved an angle of incidence (AOI) improvement of averaged absorbance reduction of 45% and 74% for AOIs of 30 and 60°, compared to that of the bare substrate. Consequently, the AR pattern layer showed excellent broadband and omnidirectional AR properties, and improved the performance of the device at various AOIs. The AR pattern layer from silica nanoparticles can be a useful approach for reducing reflectance in solar devices by a simple coating process, which will contribute to higher performance of organic photovoltaic devices.

1. Introduction

Low-cost solar technologies such as organic solar cells have had limiting steps and issues, in their operational lifetimes, degradation from environmental factors, and relatively deficient photocurrent, compared to commercial silicon photovoltaics [1-3]. Recent work has shown promise for improving the long-term reliability and photovoltaic performance of organic photovoltaics by means of structural design, encapsulation, and device engineering [4,5].

As one factor that limits power conversion efficiency (PCE), surface reflection occurs when a refractive index contrast exists between the ambient medium and the substrate of solar devices [6,7]. Anti-reflective (AR) coatings are an indispensable component to reduce or supress light loss by surface reflection, and to increase the amount of light entering the substrate of devices, which can improve the photocurrent by aggrandizing light absorption in the devices [8,9]. As photovoltaic devices continue to evolve, AR coatings are also becoming an attractive method for developing its better properties.

Generally, AR coatings are classified as single layer and multiple layer, and are intended to reduce light loss by reflection. The AR coatings have been fabricated by thin film coating of low refractive by nano-imprinting for structures, such as moth eye, that needed an additional process [11]. Among them, the hollow silica coatings have the advantages of adhesion resistance, good durability, and a low refractive index [12,13]. Surface reflection also increases significantly as the angle of in-

index material, such as MgF₂ and SiO₂-TiO₂ core shell [10], or formed

cidence (AOI) of light deviates from the normal direction, because diffuse light is scattered by the atmosphere [14]. Surface reflection by receiving oblique light must be minimized and optimized for the substrates of solar devices.

In this research, we report on the fabrication of an AR pattern layer via spin-coating of hollow silica nanoparticles on an organic photovoltaic device. We demonstrate the viability and AR effects of the AR pattern layer by transmittance measurements and measuring the PCE of the device as compared to that of a bare substrate. Moreover, we conducted absorption measurements and electrical analyses of devices with and without AR pattern at various AOIs. The results indicated that the AR pattern not only improved light absorption, but also increased omnidirectional AR effects over bare substrate for application in organic photovoltaic devices.

https://doi.org/10.1016/j.orgel.2017.11.043







^{*} Corresponding author.

E-mail address: king0401@cau.ac.kr (D.H. Wang).

¹ W. Jang and K.H. Park contributed equally to this work.

Received 2 October 2017; Received in revised form 28 November 2017; Accepted 29 November 2017 Available online 05 December 2017 1566-1199/ © 2017 Elsevier B.V. All rights reserved.

2. Experimental methods

2.1. Synthesis of anti-reflective coating material based on hollow silica nanoparticles

The silver nanoparticles were synthesized according to our previous research [15]. The dispersion (4.70 ml) of silver nanocrystals (4.7 mg), PVP (0.25 ml of 0.94 M in ethanol, Mw: 29 000), ammonium hydroxide solution (0.20 ml, 28%) and TEOS (0.12 ml) were mixed with stirring at room temperature for 30 min. After the reaction, the product was centrifuged and washed with ethanol, repeatedly. We then selectively etched the silver nanocrystal core with nitric acid to form a hollow structure. For the preparation of 0.77 ml of TEOS, 3.5 ml of (3-glycidoxypropyl) trimethoxysilane (GPTMS), 1.2 ml of methanol, 90 ml of the hollow silica dispersion (2 wt%), 0.065 ml of acetic acid, and 1 ml of deionized water were mixed by stirring at room temperature for 3 h, and 2.6 ml of methanol and 1.9 ml of 2-methoxy ethanol were then added into the solution. The anti-reflective coating solution was spin-coated onto the oxygen-plasma-cleaned glass substrate at 1000 rpm for 40 s and cured at 120 °C for 2 h.

2.2. Device fabrication and characterization

The photovoltaic cells were fabricated on the ITO-glass substrate. The substrates were prepared by washing with detergent and by sonication with water, acetone, and isopropanol. After cleaning, we formed the anti-reflective pattern onto the substrate by the method mentioned. In order to form PEDOT:PSS film on the surface, we treated the ITO by UV-ozone for 20 min, and then poly(3,4-ethylenedioxylenethiophene):poly(stylenesulf-onate) (PEDOT:PSS) (AI 4083) holetransporting material was spin-coated on top of the ITO surface (thickness of \sim 40 nm). The substrate was dried at 140 °C for 10 min. To prepare the PTB7:PC71BM solution, PTB7:PC71BM in a weight ratio of 1:1.5 at a concentration of 25 mg/ml was added to chlorobenzene (CB) without 1,8-diiodooctane (DIO) and with DIO (3 vol.%). After the active layer was formed on the PEDOT:PSS layer, a titanium oxide (TiO_x) layer with ~ 10 nm thickness was then spin-coated onto the active layer as an electron-transport layer. Subsequently, a metal cathode (Al) was deposited with a thickness of ~100 nm under a pressure of 4.0×10^{-6} Torr, using a thermal evaporator.

The cross-sectional image was observed by transmission electron microscopy (TEM) (JEM-ARM 200F). The electrical performance of the organic solar cells was measured using a solar simulator with Air Mass 1.5 Global (AM 1.5 G) at an intensity of 100 mW/cm², and the current density-voltage characteristics of the solar cells were measured using ZIVE SP1. The total cell area was 0.118 cm². After power calibration (ABET technologies, Inc., LS150, USA) with a mono-chromator (Dongwoo Optron Co., Ltd., MonoRa-500i, Korea), the incident photon-to-current efficiency (IPCE) spectra of the solar cells were calculated in order to demonstrate the short-circuit current of J_{sc} related to the *J-V* curves. Transmittance spectra and absorption spectra of the active layer were taken (Biomate 3S UV–Vis Spectrophotometer, Thermoscientific, USA).

3. Results and discussion

The organic solar cell, with AR pattern, is schematically shown in Fig. 1(a). The structure of the device from top to bottom, in order, is the patterned substrate, ITO, PEDOT:PSS, PTB7:PC₇₁BM BHJ, TiO_x, and Al electrode. The AR pattern is directly formed, as a single layer, onto the glass substrate by spin-coating of hollow silica, which is a relatively simple process. The mean diameter and shell thickness of the hollow silica are around 45 nm and 5 nm, respectively. We fabricated a device based on a bare glass substrate in order to compare it with the device with AR patterned substrate. Detailed information on this can be found in the Experimental section. In Fig. 1(b) and (c), the AR patterned

substrate was clearly seen and was not scattered under the light, whereas the image of the bare substrate revealed the scattered marks on the surface.

The completed structure of the single-layer AR pattern based on hollow silica nanoparticles on glass substrate is shown in the crosssectional TEM image of Fig. 2. From this image, we confirmed the formation of the single-layer hollow silica pattern onto the substrate. The layer thickness can be measured to be around 80 nm. Generally, AR effects are achieved by destructive interference between light reflected from the pattern-substrate and the air-pattern interfaces. Minimum reflection (R_m) from the AR pattern layer was given by the Fresnel equation:

$$R_m = \left(\frac{n_p^2 - n_a n_s}{n_p^2 + n_a n_s}\right)^2$$

where $n_{\rm p}$, $n_{\rm a}$, and $n_{\rm s}$ are the refractive indices of the AR pattern layer, air, and substrate, respectively [16]. From this equation, in order to reveal the AR effects, the AR pattern layer should have a lower refractive index than the glass substrate. The AR pattern layer on the substrate will have a lower refractive index because of the air cavities in the hollow silica nanoparticles and the empty space between pattern and substrate [16,17]. So, the reflective index of the AR pattern layer by hollow silica can be calculated using the volume fraction of air and silica as follows:

$$n_p = n_{silica} \times f_{shell} + n_a \times (f_{cavities} + f_{empty space})$$

where the refractive indices of silica (n_{silica}) and air (n_a) are 1.46 and 1.0, respectively [12]. From the TEM image in Fig. 2, a distinct fraction of air and silica can readily be identified. The reflective index of the AR pattern layer was calculated from the fraction values. We could estimate the refractive index of the AR pattern layer as being around 1.10, which is still lower than the refractive index of glass (1.50–1.70). Thus, the AR pattern layer can reduce the reflectance in the substrate.

In order to evaluate the performance of the AR pattern at the normal incidence of light, we measured the transmittance of the bare and the AR patterned substrates for the wavelength range 420–1000 nm, as shown in Fig. 3. The AR patterned substrate revealed over 90% transmittance in all regions and improved the transmittance compared to the bare substrate (under 85%). We confirmed that the AR pattern can remarkably increase transmittance because of the reflectance in the substrate [18].

Fig. 4 and Table 1 exhibit the J-V characteristics of the PTB7:PC₇₁BM BHJ device with AR nanopattern: PCE = 6.53%, $V_{\rm oc} = 0.74$ V, $J_{\rm sc} = 13.41$ mA/cm², and FF = 66%. The efficiency of the BHJ device without the pattern was 6.00%. The origin of the performance increase of the device with AR coating is the critical improvement of the $J_{\rm sc}$ from 12.30 to 13.41 mA/cm², which contributes about 10% toward the increase of the PCE. The AR pattern caused increased light absorption by low reflectance onto the surface of the substrate, which can possibly produce better charge generation [19]. Thus, we attribute our improved $J_{\rm sc}$ value to the effects from the improved optical absorption.

In order to compare the photo-activated current of the device without and with the AR pattern, we investigated the photocurrent density $(J_{\rm ph})$ as a function of internal voltage $(V_{\rm int})$ of the devices. $J_{\rm ph}$ was calculated as $J_{\rm ph} = J_{\rm L}J_{\rm D}$, where $J_{\rm L}$ and $J_{\rm D}$ are the current densities under illumination and in the dark, respectively. $V_{\rm int}$ is calculated as $V_{\rm int} = V_{\rm BI}V_{\rm appl}$, where $V_{\rm BI}$ is the built-in voltage at which $J_{\rm ph}$ is zero, and $V_{\rm appl}$ is the applied voltage. $J_{\rm ph}$ increases in proportion to voltage at low $J_{\rm ph}$, but $J_{\rm ph}$ saturates at high $V_{\rm int}$, as shown in Fig. 5 [20]. Thus, we can speculate that all carriers are collected at the electrodes in the saturated region. The saturated photocurrent ($J(_{\rm ph,sat})$) of the device with AR substrate (14.47 mA/cm²) is higher that of the device without the pattern (13.24 mA/cm²), which is proportional to the carrier generation and related to light absorption [21]. And the maximum exciton

Download English Version:

https://daneshyari.com/en/article/7700663

Download Persian Version:

https://daneshyari.com/article/7700663

Daneshyari.com